Model for the Fingering Instability of Spreading Surfactant Drops

S. M. Troian, E. Herbolzheimer, and S. A. Safran

Corporate Research Laboratories, Exxon Research and Engineering Company,
Route 22 East, Annandale, New Jersey 08801

We show that the Marangoni effect drives the fingering instability observed at the edge of an aqueous surfactant drop spreading on a thin film of water. A calculation of the unperturbed flow profile demonstrates that the spreading of the drop is controlled by the dynamics of a thin layer which develops in front of the drop. The surface-tension gradient in this region leads to the fingering instability via a mechanism mathematically similar to that in Hele-Shaw flow despite the very different underlying physics.

PACS numbers: 47.20.Dr, 68.10.Gw, 68.15.+e

We recently reported experimental results[1] on a hydrodynamic instability, first described by Marmur and Lelah,[2] which occurs when a water drop containing surfactant spreads on a smooth glass surface premoistened with a thin water film. Upon deposition of the drop on the substrate, liquid in the thin water film is swept away from the vicinity of drop causing thinning of the film near the drop edge while a thickened corona, similar to a shock front, travels away from the drop. As this profile develops, the drop rapidly spreads into the thinned region and begins propagating fingers from the spreading front. Although the instability we observe leads to fingering patterns similar to those arising in Hele-Shaw flow, dendritic growth, and systems related to diffusion-limited aggregation, the reason for this has been unclear until now since our system has no externally applied driving force for the flow nor is it controlled by diffusive phenomena.

Experimentally, the rapid spreading and fingering depend on the initial surfactant concentration and the thickness of the initial water film which strongly suggests that the instability is driven by the Marangoni effect.[3] Surface-tension gradients, established in our experiments by spatial variations in surfactant concentration at the air-liquid interface, cause a traction along the interface which induces flow in the direction of increasing surface tension (i.e., in the direction of decreasing surfactant concentration). While the Marangoni effect has been studied in a broad range of situations leading to both stable and unstable flows,[4,5] these experiments indicate a new instability which occurs at the *spreading front* of a drop.

We first calculate the time evolution of the *unperturbed* flow profile for a surfactant-coated drop spreading on a preexisting thin viscous layer of the same fluid but free of surfactant. Using asymptotic analysis, we show that the Marangoni effect leads to the formation of a long thin region ahead of the macroscopic drop in which a surfactant-concentration gradient is established. The concentration gradient produced in this region controls the spreading velocity of the drop and leads to a

new spreading behavior which is independent of the apparent contact angle in the drop. We then perform a linear stability analysis which shows that this flow is unstable to perturbations in the position of the moving front. Although the underlying physics is quite different, the stability analysis is mathematically similar to that for viscous fingering[6] and other "diffusion-limited" growth processes. In the present case, however, there is no apparent stabilization mechanism except at very small length scales.

Applying the lubrication approximation,[7] the Navier-Stokes equations reduce to

$$\eta \frac{\partial^2 \mathbf{u}}{\partial z^2}(x,y,z,t) = \nabla p(x,y,t), \tag{1}$$

where $\mathbf{u}$ is the fluid velocity in the plane parallel to the substrate, p is the pressure in the fluid, η is the fluid viscosity (unchanged by low surfactant concentrations), t is time, and ∇ is the gradient in the x-y plane. In this thin-film approximation, the pressure is constant in the z direction (the direction perpendicular to the solid surface) and is therefore equal to the capillary pressure at the surface of the fluid which for small slopes is $p = -\sigma \nabla^2 h$, where $z = h(x,y,t)$ defines the free surface of the fluid layer and $\sigma(x,y,t)$ is the local surface tension.

It is convenient to view the flow from a reference frame attached to the edge (cf. region 4 in Fig. 1) of the spreading drop which moves with speed $\mathbf{U}_{\mathrm{ref}}(t)$, to be determined later self-consistently. In this frame the boundary conditions are (i) the no-slip condition for the fluid at the solid surface, $\mathbf{u}(x,y,z=0,t) = -\mathbf{U}_{\mathrm{ref}}(t)$, and (ii) the Marangoni stress condition, $\eta \mathbf{u}_z|_{z=h(x,y,t)} = \nabla \sigma = -\alpha \nabla \Gamma$, where the subscript z denotes differentiation, Γ is the surfactant concentration at the liquid surface, and $\alpha = |\partial \sigma/\partial \Gamma|$ (which we will take as a constant).

From the solution of Eq. (1) subject to the two boundary conditions, the fluid volumetric flux becomes

$$\mathbf{Q} = \int_0^h \mathbf{u}\, dz = \frac{\sigma}{12\eta} h^3 \nabla \nabla^2 h + \frac{h}{2}(\mathbf{U}_s - \mathbf{U}_{\mathrm{ref}}), \tag{2}$$
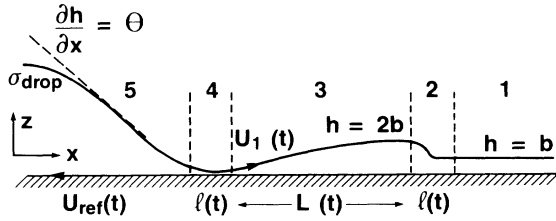
FIG. 1. Schematic of the unperturbed height profile, $h(x,t)$, for a drop of surfactant solution, with surface tension σ_{drop}, spreading on a flat surfactant-free film of liquid. Other quantities are defined in the text.

where the surface velocity, $\mathbf{U}_s(x,y,t) = \mathbf{u}(x,y,z=h,t)$, is given by

$$\mathbf{U}_s = \frac{\sigma}{2\eta} h^2 \nabla \nabla^2 h - \frac{h\alpha}{\eta} \nabla \Gamma - \mathbf{U}_{ref} . \tag{3}$$

Finally, to determine h and Γ one solves the conservation equations for the fluid volume and surfactant concentration,

$$\partial h / \partial t + \nabla \cdot \mathbf{Q} = 0 , \tag{4a}$$

$$\partial \Gamma / \partial t + \nabla \cdot (\mathbf{U}_s \Gamma) = 0 , \tag{4b}$$

with appropriate boundary and initial conditions. In the surfactant conservation equation the surfactant is assumed insoluble.

We now determine the unperturbed flow profile for the case of a 2D drop with a planar front[8] where $\mathbf{U}_{ref} = U_{ref}\hat{\mathbf{e}}_x$. As shown in Fig. 1, five distinct regions develop in the unperturbed flow profile. Region 1 is the preexisting film of height b which remains free of surfactant throughout the spreading process. Viewed in the reference frame moving with the edge of the drop, the velocity profile is uniform with $u = -U_{ref}$. In region 3, whose length $L(t)$ is initially zero but quickly increases, the fluid height remains $\sim b$ but the surfactant concentration changes from the value in the drop to zero at the boundary of region 1. The flow in this region is driven by the Marangoni effect which acts to spread the concentration jump which is established when the drop is first placed on the precursor layer. The velocity scale established by the Marangoni boundary condition dictates that the capillary-pressure terms are negligible in this region provided that $L(t)$ is large compared to b, which is true except for extremely early times. Region 5 extends over the radius of the drop, which to leading order is a spherical cap over which the surfactant concentration varies little. We characterize this region as a reservoir of fluid with asymptotic slope $\theta(t)$, and with constant surface tension σ_{drop}. In regions 2 and 4 the capillary pressure plays an important role and allows the solutions in regions 1, 3, and 5 to smoothly match to each other. The capillary-pressure terms operate on a smaller length scale than the Marangoni force and so the lengths of regions 2 and 4 are short compared to those of 3 or 5 (but

long enough that the lubrication approximation applies).

The conditions governing the growth of $L(t)$ and the layer height at $x = L(t)$ can be obtained by the matching of regions 1 and 3. Since region 2 defines the separation point between the regions with and without surfactant, no surfactant can flow in or out of region 2. Hence, viewed in a frame moving with region 2, the surface velocity at the edge of region 3 must vanish. Also, the fluid flux coming into region 2 from the uniform flow on the right must equal that flowing out in the simple shear flow on the left. Together, these two conditions require that $h(L,t) = 2b$ and

$$\frac{dL}{dt} = U_s(L,t) = -\frac{2\alpha b}{\eta} \Gamma_x(x=L) - U_{ref} . \tag{5}$$

The discontinuity in the height profile from $2b$ to b is smoothed in region 2 by the inclusion of the capillary-pressure terms, but the details play no role to leading order.

Region 4, which matches regions 3 and 5, is important in determining the spreading velocity of the drop. Because this region is much shorter than region 3, it responds relatively quickly and to leading order the fluxes of liquid and of surfactant in this region can be treated as quasisteady. Furthermore, because this region is short, the Marangoni boundary condition requires that the change in concentration across region 4 is small. The surfactant conservation equation then requires that U_s be constant in order to maintain a constant flux of surfactant from the drop to region 3. Letting l denote the length of region 4 and defining the stretched variables $H = h/h_1$ and $X = x/l$, Eq. (4a) together with the matching of the fluid flux across the boundary between regions 3 and 4 gives

$$\frac{\sigma_{drop}}{6\eta(U_{ref} - U_1)} \left[\frac{h_1}{l} \right]^3 H^3 H_{XXX} = H - 1 , \tag{6}$$

with the asymptotic boundary conditions $H(+\infty) = 1$, $H_X(+\infty) = 0$, and $H_{XX}(-\infty) = 0$. In Eq. (6), $h_1(t)$ and $U_1(t)$ are defined as the height and surface velocity of region 3 at $x = 0$. The capillary-pressure term in Eq. (6) becomes comparable to the Marangoni term when

$$\frac{h_1}{l} = \left[\frac{6\eta}{\sigma_{drop}} (U_{ref} - U_1) \right]^{1/3} . \tag{7}$$

With Eq. (7) defining l, Eq. (6) can be solved independently of any of the solutions coming from regions 3 or 5.

Matching regions 4 and 5 requires the asymptotic slope emerging from region 4 to be equal to $\theta(t)$, the slope at the edge of region 5; i.e., $\theta(t) = (h_x)_{-\infty} = (h_1/l) \times S$, where $S = H_X(-\infty)$ is obtained from the solution of Eq. (6). Substituting Eq. (7) for h_1/l and Eq. (3) to evaluate U_1, we obtain

$$\frac{dR}{dt} = U_{ref}(t) = -\frac{\alpha h_1}{2\eta} \frac{\partial \Gamma}{\partial x}(x=0) + \frac{\sigma_{drop}}{12\eta} \left[\frac{\theta(t)}{S} \right]^3 , \tag{8}$$

where $R(t)$ is the radius of the drop. Finally, conservation of the drop volume relates $\theta(t)$ to $R(t)$; e.g., for an axisymmetric spherical cap with small θ, $\theta(t) = 4V_0/\pi R^3(t)$, where V_0 is the initial volume of the drop, while for a 2D drop, $\theta(t) = 3A_0/2R^2(t)$, where A_0 is the initial volume per unit length of the drop. The entire spreading process can now be determined by solving Eqs. (4a) and (4b) for region 3 subject to Eqs. (5) and (8) which control $L(t)$ and $R(t)$.

We solved these nonlinear equations numerically[9] by finite differencing the spatial derivatives and using the program LSODE [10] to integrate implicitly the resulting ordinary differential equations in time. Figure 2 shows typical time developments of the height, concentration, and surface velocity profiles for the spreading layer in region 3 for small drops. The interesting feature, which agrees with qualitative experimental observations, is that the fluid layer, with initial uniform height $2b$ and uniform concentration gradient $\Gamma_d/L(t)$, begins to thin near the drop edge. This occurs because although the initial profiles of constant height and constant concentration gradient give constant volume flux of liquid, and hence

FIG. 2. The profiles in region 3 for the (a) height $h/2b$, (b) concentration Γ/Γ_{drop}, and (c) relative surface velocity $(U_s - U_{rel})/[L(\tau)/t_F]$, as functions of $\tau = t/t_F$, where $t_F = 72(a\Gamma_{drop}/\sigma_{drop})(\eta b/\sigma_{drop})[S/\theta(0)]^3$.

solve the steady form of Eq. (4a) for h, the constant surface velocity brings more surfactant in from the drop than can be convected away. Hence, the concentration gradient, and, therefore, the surface velocity, decrease near the drop and the liquid is pulled into the layer faster than it is supplied from the drop, thereby causing the layer to thin.

At relatively early times when $L(t)$ is small, the Marangoni terms dominate the capillary terms in Eqs. (5) and (8) and the spreading velocity is independent of the apparent contact angle in the drop. Since h and Γ change slowly compared to $L(t)$, Eqs. (5) and (8) show that both $L(t)$ and $R(t) - R(0)$ grows as $\sqrt{t}$ during this regime. For intermediate times as $L(t)$ becomes large, the capillary spreading can become comparable to the Marangoni contribution but as the drop radius increases the contact angle decreases sufficiently fast that Marangoni spreading always dominates at late times. Of course, with an insoluble surfactant, the concentration in the drop (assumed constant in these calculations) will decrease with time as the surface area of the drop and of the layer in front of the drop increase. We have found that this together with the thinning of the layer near the drop causes the $t^{1/2}$ growth to slow down at late times.

These calculations of the unperturbed spreading demonstrate that during most of the time (including when the fingers first appear) the Marangoni effect dominates the capillary force everywhere except in region 4.[11] They also confirm that a thin layer develops ahead of the drop in which a surfactant-concentration gradient, which controls the spreading rate, is established. This structure suggests that the onset of the fingering can be explained by a model in close analogy to the Saffman-Taylor instability. When the Marangoni terms are dominant, the average velocity in the fluid layer is proportional to the surfactant gradient Γ_x times a mobility factor h/η. Hence, the surfactant concentration now plays the same role as does the pressure in Hele-Shaw flow. Of course, in Hele-Shaw flow the fingering occurs because the fluid mobility behind the front is higher due to the lower viscosity there. In our problem the viscosity is uniform but the layer height is greater in the drop. Hence, the basic mechanism of fingering due to an adverse mobility gradient applies to our problem even though the detailed flow structure is much more complicated.

If we consider disturbances with wavelengths satisfying $l \ll \lambda \ll L(t)$, the onset of the fingering can be simply described by a linear stability analysis. First, although the mobility increases continuously back towards the drop, when $\lambda \gg l$ the disturbances propagate far enough into the drop that the typical mobility there is large compared to that in the layer ahead of the drop. Consequently, on the scale of l we can treat the edge of the drop as a sharp front separating a region of large mobility from one of low mobility. Second, for disturbances with $\lambda \ll L(t)$, the base flow profiles in region 3 evolve on
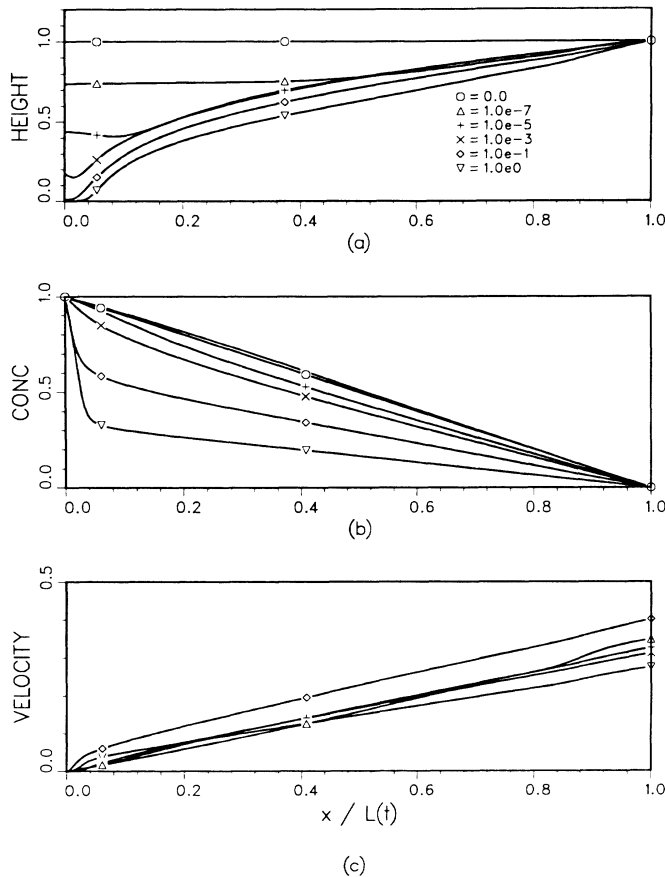
time and length scales which are slow compared to those appropriate to the perturbations. Consequently, within the framework of multiple-scales analysis,[12] the base flow variables can be treated as constants and Eqs. (4a) and (4b) governing the disturbances have quasiconstant coefficients.

We consider disturbances caused by a corrugation in the position of the edge of the drop given by $\tilde{x}(t) = Ae^{\omega t + iqy}$, where $A \ll 1$, ω is the growth constant, and q is the wave number of the disturbance. The unperturbed flow variables in region 3 are denoted by h and Γ, while the disturbances are represented by $\tilde{h}e^{\omega t + \beta x + iqy}$ and $\tilde{\Gamma}e^{\omega t + \beta x + iqy}$, where only spatially decaying (i.e., $\beta < 0$) solutions are physical. Two boundary conditions must be imposed at the undulating front: (i) The surfactant concentration equals that in the drop, and (ii) the front velocity equals the average fluid velocity given by Eq. (8). By expanding the flow variables in a Taylor series about the unperturbed front position, these conditions require that $\tilde{\Gamma}(0) = -A\Gamma_x(0)$ and

$$\omega = -(\alpha/2\eta)[\beta h\tilde{\Gamma} + \tilde{h}\Gamma_x + h_x\Gamma_x + h\Gamma_{xx}]_{x=0}. \qquad (9)$$

$\tilde{h}$ and β are found by solving the linearized form of Eqs. (4a) and (4b) in region 3. For the large-q limit (i.e., for $q \gg L^{-1}$) being considered here, we find that $\beta = -q - h_x/h + o(1)$ and $\tilde{h}/\tilde{\Gamma} = -h/\Gamma + h_x/\Gamma_x$. Substituting these results into Eq. (9) yields

$$\omega = -(\alpha/2\eta)[qh\Gamma_x + h\Gamma_x^2/\Gamma + h\Gamma_{xx}]_{x=0}. \qquad (10)$$

Hence, for wavelengths which are short compared to the length of region 3 (i.e., for large q), the first term in Eq. (10) dominates and since $(d\Gamma_0/dx)_{x=0} < 0$ (cf. Fig. 2), $\omega > 0$ and the flow is always unstable. We emphasize that to leading order in the large-q limit the disturbance concentration satisfies Laplace's equation and the perturbations in the height are negligible. Consequently, the analogy to the Saffman-Taylor instability is complete in this limit.

While the onset of the instability can be explained in close mathematical analogy to Saffman-Taylor fingers, the stabilizing mechanism and the nonlinear evolution of the fingers are expected to be different. There is no surface tension in this problem associated with curvature of the front, $d^2\tilde{x}/dy^2$, since the drop edge is not a boundary between immiscible fluids. One stabilizing mechanism is the surface tension associated with the curvature of the air-liquid interface, d^2h/dy^2, but inclusion of these terms in the above analysis shows that they affect the growth rate only for wavelengths which are much smaller than the size of region 4. On these short length scales the above model breaks down since the disturbances do not penetrate far enough into the drop to allow a significant mobility difference to be operative. Simple surface diffusion of surfactant is too slow to affect the fingering, but transfer of soluble surfactant from the liquid layer to the interface may be important. These effects need to be considered in more detail.

---

[1]S. M. Troian, X. L. Wu, and S. A. Safran, Phys. Rev. Lett. 62, 1496 (1989).

[2]A. Marmur and M. D. Lelah, Chem. Eng. Commun. 13, 133 (1981).

[3]V. G. Levich and V. S. Krylov, Annu. Rev. Fluid Mech. 1, 293 (1969).

[4]M. S. Borgas and J. B. Grotberg, J. Fluid Mech. 193, 151 (1988), and references therein.

[5]J. R. A. Pearson, J. Fluid Mech. 4, 489 (1958).

[6]P. G. Saffman and G. I. Taylor, Proc. Roy. Soc. London A 245, 312 (1958).

[7]G. K. Batchelor, An Introduction to Fluid Dynamics (Cambridge Univ. Press, Cambridge, 1967).

[8]The analysis is identical for axisymmetric drops except, of course, that the divergence operator in the continuity equations contains extra terms involving the radius. These complications modify slightly the evolution of the profiles in region 3 but introduce no new physics. Since the onset of the instability occurs at early times, the prediction for the onset of instability obtained below is identical for axisymmetric and 2D drops.

[9]S. M. Troian, E. Herbolzheimer, and S. A. Safran (to be published).

[10]A. C. Hindmarsh, Livermore Solver for Ordinary Differential Equations (Lawrence Livermore Laboratory, Livermore, 1980).

[11]Calculations coupling the evolution of region 3 with the development of the height and concentration profiles in the drop have confirmed that the assumptions of a spherical cap shape and almost constant concentration across the drop remain valid even when the Marangoni terms dominate the capillary terms in the drop region (Ref. 9). This results because the fluid mobility for the Marangoni flow, h/η, is large in the drop compared to region 3. Consequently, a much smaller concentration gradient is needed in the drop in order to maintain comparable surface velocities in the two regions.

[12]C. M. Bender and S. A. Orszag, Advanced Mathematical Methods for Scientists and Engineers (McGraw-Hill, New York, 1978).